J|A|C|S COMMUNICATIONS

Published on Web 04/28/2010

Localization of *p*-Nitroaniline Chains Inside Zeolite ZSM-5 with Second-Harmonic Generation Microscopy

Monique A. van der Veen,[†,‡] Bert F. Sels,[†] Dirk E. De Vos,*[,†] and Thierry Verbiest*[,‡]

Department of Microbial and Molecular Systems, Centre for Surface Chemistry and Catalysis, Kasteelpark Arenberg 23, and Department of Chemistry, Celestijnenlaan 200D, Katholieke Universiteit Leuven, B-3001 Leuven, Belgium

Received February 24, 2010; E-mail: dirk.devos@biw.kuleuven.be; thierry.verbiest@fys.kuleuven.be

Second-harmonic generation microscopy (SHGM) has recently emerged as a powerful tool for high-contrast study of cellular structures,[1] but it has hardly been applied in materials science.[2] Here we report the first SHGM study of a zeolite and elucidate the molecular organization of *p*-nitroaniline (PNA) in the pore system of zeolite ZSM-5 in relation to its SHG response.

SHG from PNA-filled zeolites can be observed only if there is a net non-centrosymmetric arrangement of PNA. For example, in the unidimensional pores of AlPO-5 (AFI topology), PNA forms strings that are organized in a head-to-tail fashion.[3] PNA in ZSM-5 (MFI topology) also gives a strong SHG,[3b,4a] but solid-state NMR and X-ray diffraction investigations indicate that PNA is disordered inside the pore system,[4] which seems hard to reconcile with the SHG result. To this is added the structural complexity of ZSM-5 crystals with varying shape, aspect ratio, and defect content. Better insight into ZSM-5 crystal structure has recently been achieved by combined use of fluorescence microscopy, atomic force microscopy (AFM), and electron backscatter diffraction (EBSD).[5] In rare cases, "coffin-shaped" MFI crystals have a uniform crystallographic orientation all over the crystallite, even if various pyramidal and wedge-shaped components can be readily distinguished (Scheme 1a).[6] However, the crystal components below the (010) planes frequently undergo a 90° rotation around the *c*-axis (Scheme 1b). As will be shown, space-resolved observation of SHG is crucial for understanding the complex organization of PNA in ZSM-5.

First, coffin-shaped ZSM-5 crystals with a typical aspect ratio of 7 were selected (sample A, Si/Al = 700). Previous AFM characterization has shown that the step size of the terraces on (010), viz. ~20 nm, is distinctly larger than on (100), viz. <5 nm.[7] Such difference in step heights on the crystal surfaces proves that the crystallographic axis orientation is identical all over the crystal (Scheme 1a), without the 90° intergrowth commonly observed for ZSM-5.[6] After the samples were loaded with PNA for 24 h at 110 °C, thermogravimetric analysis (TGA) revealed a PNA loading of 11 ± 1 wt %, or 5.2 molecules per unit cell.

In our SHG microscope, we illuminate the sample with polarized light under normal incidence in a transmission geometry. In such a configuration, dipolar chains of PNA parallel with the propagation of light will not generate SHG, and only the dipole chains in the sample plane will be visualized. Second-harmonic generation can be described by the different components of the nonlinear polarization $P_i(2\omega)$ at frequency 2ω:

$$P_i^{(2)} = \sum_{j,k} \chi_{ijk}^{(2)} E_j E_k$$

with $\chi_{ijk}^{(2)}$ a component of the second-order susceptibility tensor and $E_{j,k}$ the electric field component of the incoming light.

The number of independent susceptibility components is highly dependent on the symmetry of the system, and the particular components that are addressed will depend on the experimental geometry. In our measurements, only three nonvanishing components are addressed: $\chi_{xxx}^{(2)}$, $\chi_{xyy}^{(2)}$, and $\chi_{yxy}^{(2)} = \chi_{yyx}^{(2)}$.[8] Furthermore, the values of these components will be different, depending on whether the molecules are arranged in a linear or a zigzag array, and this affects the dependence of the SHG light on the incident light polarization.

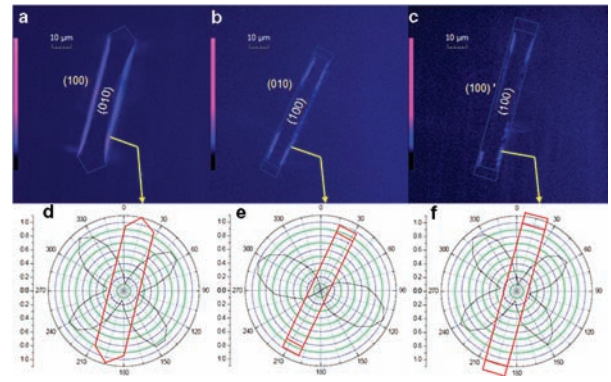

Figure 1. SHG images (a−c) and polarization patterns (d−f) for PNA-loaded ZSM-5: (a,d) crystal A1 from batch A, lying on (010); (b,e) crystal A2 from batch A, lying on (100); (c,f) crystal from batch B, lying on (100).

Scheme 1

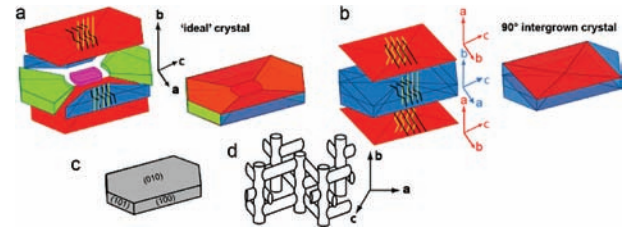

Figure 1a,b shows the SHG of two PNA-filled ZSM-5 crystals from sample A. They are positioned with their (010) face (crystal A1) and their (100) face (crystal A2) respectively in the *xy*-plane. SHG signals are only found in narrow rims at the crystal border, close to the (100) outer faces of the crystal (Figure 1a), or close to the (010) outer faces (Figure 1b). In the former case, these rims get narrower toward the crystal ends, suggesting that the pyramidal components of the crystal under the (100) faces (shown in blue in scheme 1a) delimit the SHG-active zone. For the SHG-active areas, we recorded the dependence of SHG on the polarization angle of the linearly polarized input light (Figure 1d,e). The two strips along crystal A1 show everywhere a four-lobe polarization pattern. By contrast, the SHG from the strips close to (010) of crystal A2 follows a two-lobe polarization pattern, with maximum intensity along the *b*-axis of the crystal. Both polarization patterns are clearly different, which indicates that the orientation of

[†] Department of Microbial and Molecular Systems.
[‡] Department of Chemistry.

 10.1021/ja101614w

PNA is different in both cases. The two-lobe pattern, in which the minimum intensity approaches zero, corresponds with straight dipole chains of PNA; the clearly distinct four-lobe pattern can be modeled on the basis of zigzag dipole chains of PNA (see Supporting Information). This orientation is consistent with the (010) surface faces giving access to the straight pores and (100) faces to the sinusoidal pores, at least in this particular ZSM-5 crystal with uniform axis orientation throughout the crystallite. It is also clear that oriented dipole chains are formed only in pores that are directly accessible from the outer surface; for instance, for crystal A1, no SHG signal generated by zigzag PNA chains is detected in the middle of the (010) plane, where the sinusoidal pores run under and parallel to the surface (see Supporting Information and the red components in Scheme 1a). This agrees with the earlier hypothesis of "surface selection": the zeolite prefers one end of PNA over the other as it enters the crystal.[3,4a]

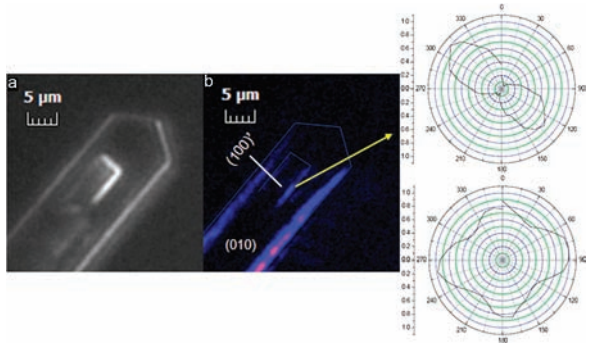

Figure 2. Small ramp on the (010) face of ZSM-5: (a) optical image; (b) SHG image and corresponding polarization patterns.

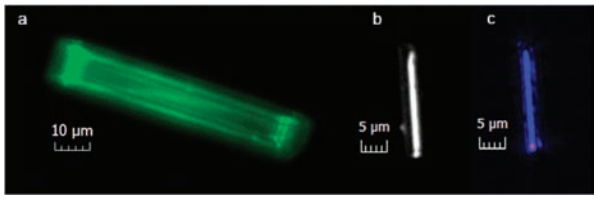

Figure 3. (a) Two-photon fluorescence image of a PNA-filled ZSM-5 crystal. (b,c) Optical and SHG images of PNA-filled SAPO-5 crystal.

Figure 1c shows a crystal from a different batch B, with Si/Al = 40, positioned on its (100) face. In this batch, we previously found a large extent of 90° intergrowth covering the original (010) crystallographic faces.[5a,c,7] After PNA loading, SHG is again apparent near the (010) faces, but with a different polarization pattern (Figure 1f vs 1d): the four-lobe pattern of zigzag-organized PNA now clearly indicates that a 90° axis rotation has occurred under the hexagonal crystal face, which therefore must be considered as a (100)′ face. The latter gives access to sinusoidal pores. Even smaller defects can be visualized in detail. In Figure 2, a small ramp is seen protruding from the (010) face. Mapping of SHG polarization signatures reveals the four-lobe signature of sinusoidal channels at the outer contours of the mother crystal, whereas the lateral faces of the ramp display the two-lobe straight channel signature, which directly proves a 90° rotation.

In all ZSM-5 samples, SHG is observed only near the outer crystal surface. This is surprising, since both TGA and the two-photon fluorescence image in Figure 3a indicate that PNA fills the pores to a large extent, and in a fairly homogeneous fashion. Apparently, only close to the outer surface do the PNA molecules have a sufficient head-to-tail organization, not only with identical direction but also with the same sense. The bidirectional MFI pore system plays a crucial role here. As the PNA diffusion front moves into the ZSM-5 crystal, e.g. starting from (010), through the straight channel, there is an increasing chance that a PNA molecule jumps to a neighboring straight channel via a sinusoidal connecting channel (see Scheme 1d). The electrostatic forces between PNA molecules in a string are rather weak, as they are proportional with $1/r^3$. Therefore, a newly intruding PNA molecule could assume both the parallel and the antiparallel orientations, even if not necessarily with the same probability. In the latter case, the dipolar alignment is weakened, and this eventually leads to loss of the SHG signal. The more pronounced disorder of PNA organization in the crystal interior is in fact in perfect agreement with NMR and XRD data.[4] A disturbance of PNA organization is less likely close to the surface, since the higher degree of pore occupation with PNA during diffusion makes hopping of a PNA molecule to an adjacent channel less probable. This explains the SHG response at the crystal edges.

If this hypothesis is correct, a one-dimensional SAPO-5 crystal, extensively filled with PNA, should have dipole chains and SHG over the full crystal length. This is convincingly borne out by Figure 3c. Thus, the unidimensional nature of the pores makes it much easier to keep the arrays of PNA organized. Note that the 12-MR pores of SAPO-5 are too narrow to allow a head-to-tail tumbling of PNA. These results are in accordance with those of Herance et al., who showed that the SHG efficiency of PNA-loaded zeolites is significantly higher for one-dimensional pore architectures than for two-dimensional pore systems.[9]

Summarizing, SHG microscopy is a powerful tool for revealing structural details of zeolites and allows the molecular organization of *p*-nitroaniline in complex ZSM-5 crystals to be related to their SHG response.

Acknowledgment. M.A.v.d.V. is a research assistant of FWO (Belgium). We thank Jasper Van Noyen for synthesis of the SAPO-5 sample. We thank K.U. Leuven (CASAS Methusalem and INPAC grants) and IAP project 6/27 (Belgium).

Supporting Information Available: SHGM setup, sample characteristics, polarization dependency of SHG light, note on SHG of the different section of ZSM-5, and complete ref 5b. This material is available free of charge via the Internet at http://pubs.acs.org.

References

(1) Mertz, J. *Curr. Opin. Neurobiol.* **2005**, *14*, 610.
(2) (a) Zavelani-Rossi, M.; Celebrano, M.; Biagioni, P.; Polli, D.; Finazzi, M.; Duo, L.; Cerullo, G.; Labardi, M.; Allegrini, M.; Grand, J.; Adam, P.-M. *Appl. Phys. Lett.* **2008**, *92*, 093119/1. (b) Chen, I.-H.; Chu, S.-W.; Bresson, F.; Tien, M.-C.; Shi, J.-W.; Sun, C.-K. *Opt. Lett.* **2003**, *28*, 1338.
(3) (a) Caro, J.; Finger, G.; Kornatowski, J.; Richter-Mendau, J.; Werner, L.; Zibrowius, B. *Adv. Mater.* **1992**, *4*, 273. (b) Werner, J.; Caro, J.; Finger, G.; Kornatowski, J. *Zeolites* **1992**, *2*, 658. (c) Marlow, F.; Wübbenhorst, M.; Caro, J. *J. Phys. Chem.* **1994**, *98*, 12315. (d) Klap, G. J.; van Klooster, S. M.; Wübbenhorst, M.; Jansen, J. C.; van Bekkum, H.; van, Turnhout *J. Phys. Chem. B* **1998**, *102*, 9518. (e) Klap, G. J.; Wübbenhorst, M.; Jansen, J. C.; van Koningsveld, H.; van Bekkum, H.; van Turnhout, J. *Chem. Mater.* **1999**, *11*, 3497.
(4) (a) Reck, G.; Marlow, F.; Kornatowski, J.; Hill, W.; Caro, J. *J. Phys. Chem.* **1996**, *100*, 1698. (b) van Koningsveld, H.; Koegler, J. H. *Microporous Mater.* **1997**, *9*, 71. (c) Mentzen, B. F.; Lefèbvre, F. *J. Chim. Phys.* **1998**, *95*, 1052. (d) Fyfe, C. A.; Brouwer, D. H. *Microporous Mesoporous Mater.* **2000**, *39*, 291.
(5) (a) Roeffaers, M. B. J.; Ameloot, R.; Baruah, M.; Uji-i, H.; Bulut, M.; De Cremer, G.; Müller, U.; Jacobs, P. A.; Hofkens, J.; Sels, B. F.; De Vos, D. E. *J. Am. Chem. Soc.* **2008**, *130*, 5763. (b) Karwacki, L.; et al. *Nat. Mater.* **2009**, *8*, 959. (c) Roeffaers, M. B. J.; Ameloot, R.; Bons, A. J.; Mortier, W.; De Cremer, G. J.; de Kloe, R.; Hofkens, J.; De Vos, D. E.; Sels, B. F. *J. Am. Chem. Soc.* **2008**, *130*, 13516.
(6) Agger, J. R.; Hanif, N.; Cundy, C. S.; Wade, A. P.; Dennison, S.; Rawlinson, P. A.; Anderson, M. W. *J. Am. Chem. Soc.* **2002**, *125*, 830.
(7) Roeffaers, M. B. J.; Sels, B. F.; Uji-i, H.; Blanpain, B.; L'hoëst, P.; Jacobs, P. A.; De Schryver, F. C.; Hofkens, J.; De Vos, D. E. *Ang. Chem. Int., Ed.* **2007**, *46*, 1706.
(8) Verbiest, T.; Clays, K.; Rodriguez, V. *Second-order nonlinear optical characterization techniques, an introduction*; CRC Press: Boca Raton, 2009.
(9) Herance, J. P.; Das, D.; Marquet, J.; Bourdelande, J. L.; García, H. *Chem. Phys. Lett.* **2004**, *395*, 186.

JA101614W